

# Xray observations of high redshift radio galaxies

C.L. Carilli <sup>a</sup>

<sup>a</sup>*NRAO, Socorro, NM, USA*

---

## Abstract

I summarize Xray properties of high redshift radio galaxies, beginning with a brief review of what has been learned from Xray observations of low redshift powerful radio galaxies (in particular, Cygnus A), and then turning to Chandra observations of four high redshift radio galaxies. Hot Xray emitting atmospheres of the type seen in low redshift clusters are not detected in the high redshift sources, suggesting that these systems are not yet virialized massive clusters, but will likely evolve into such. Xray emission from highly obscured AGN is detected in all cases. Extended Xray emission is also seen, and the extended emission is clearly aligned with the radio source, and on a similar spatial scale. Multiple mechanisms are proposed for this radio-Xray alignment, including inverse Compton scattering of photons from the AGN (the 'Brunetti mechanism'), and thermal emission from ambient gas that is shocked heated by the expanding radio source. The pressure in the high filling factor shocked gas is adequate to confine the radio source and the low filling factor optical line emitting clouds.

*Key words:* galaxies: active – galaxies: high-redshift – radio continuum: galaxies – Xrays: galaxies, cluster

---

## 1 Introduction

There are a number of possible Xray emission mechanisms for high redshift radio galaxies. Thermal emission from hot gas probes the large scale gas distribution and the hydrodynamic interaction between the expanding radio source and this gas. Thermal and/or non-thermal emission from the AGN, and soft Xray absorption toward the AGN, can be used to study physical processes in the AGN and conditions in the local AGN environment. Non-thermal emission from radio jets (synchrotron and/or inverse Compton (IC)) can be used to constrain the relativistic particle acceleration and loss mechanisms, and the source magnetic fields. Most recently, detection of Xray emission from (likely)

cluster members in one high  $z$  radio galaxy has revealed the (obscured) AGN population in the associated proto-cluster.

This paper summarizes what has been learned from Xray observations of lower redshift radio galaxies, and then reviews observations of higher redshift sources. Particular attention is paid to the source PKS1138-262 at  $z=2.2$ , which shows evidence for most of the phenomena discussed above, and to the radio-Xray 'alignment' seen in this, and other, high redshift radio galaxies. I use  $H_o = 65 \text{ km s}^{-1} \text{ Mpc}^{-1}$  and a flat cosmology with  $\Omega_m = 0.3$  throughout.

## 2 Xray observations of low redshift radio galaxies

The high redshift radio galaxies discussed below are all very high luminosity sources, with  $P_{178\text{MHz}} > 5 \times 10^{28} \text{ W Hz}^{-1}$ . The only radio source at  $z < 0.4$  with comparable luminosity is Cygnus A at  $z = 0.057$  (Carilli & Barthel 1996). Cygnus A has been extensively studied in the Xray, and displays most of the thermal and nonthermal emission phenomena discussed above (Harris et al. 1994; Carilli et al. 1994). In this section I will use the recent high resolution Chandra images of Cygnus A (Wilson et al. 2000; Smith et al. 2002; Young et al. 2002) to illustrate these various phenomena.

### 2.1 *Thermal emission and hydrodynamics*

The Cygnus A radio source is situated at the center of a dense cluster atmosphere that extends to a radius of at least 0.5 Mpc (Smith et al. 2002). The total Xray luminosity of the cluster is  $L_{2-10\text{keV}} = 1.4 \times 10^{45} \text{ erg s}^{-1}$ , at an average temperature of 8 keV, and the electron density at the radio hot spot radius (70 kpc)  $= 0.006 \text{ cm}^{-3}$  (Ueno et al. 1994; Reynolds & Fabian 1996). The total gas mass is  $2 \times 10^{13} M_\odot$  and the total gravitational mass is  $2 \times 10^{14} M_\odot$  (Reynolds & Fabian 1996).

The hydrodynamic evolution of a light, hypersonic jet propagating into a hot intercluster medium (ICM) has been considered in detail by many authors (see the contribution by Bicknell in these proceedings). The standard model involves a double shock structure, with a terminal jet shock and a stand-off, or bow, shock propagating into the external medium (see Figure 1A). The two shocked fluids (jet and external) meet in pressure equilibrium along a contact discontinuity. The radio emission is thought to be from shocked jet material contained within the contact discontinuity.

A number of signatures in Xray images are expected from such a system,

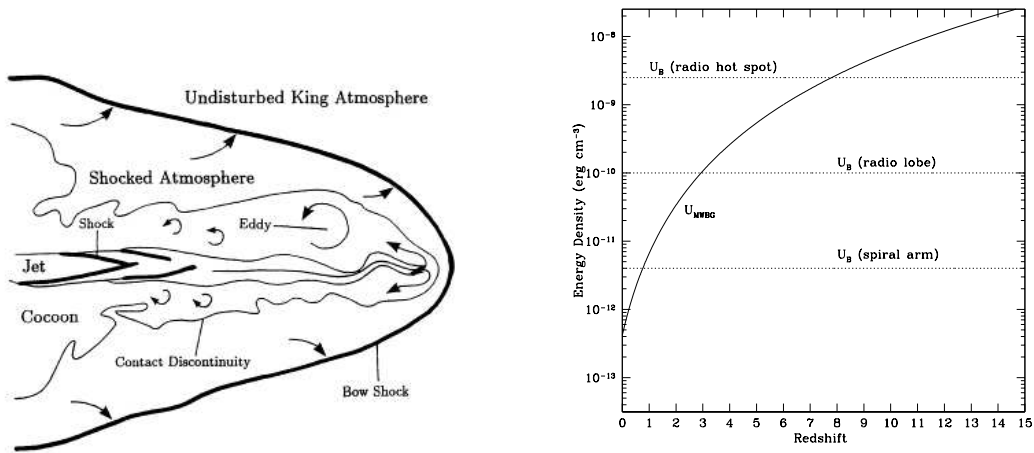


Fig. 1. A. The figure on the left shows a heuristic model for the hydrodynamic evolution of a light, hypersonic jet (Clarke et al. 1997). B. The figure on the right show the evolution with redshift of the energy densities in the CMB compared to the magnetic energy densities in different cosmic structures.

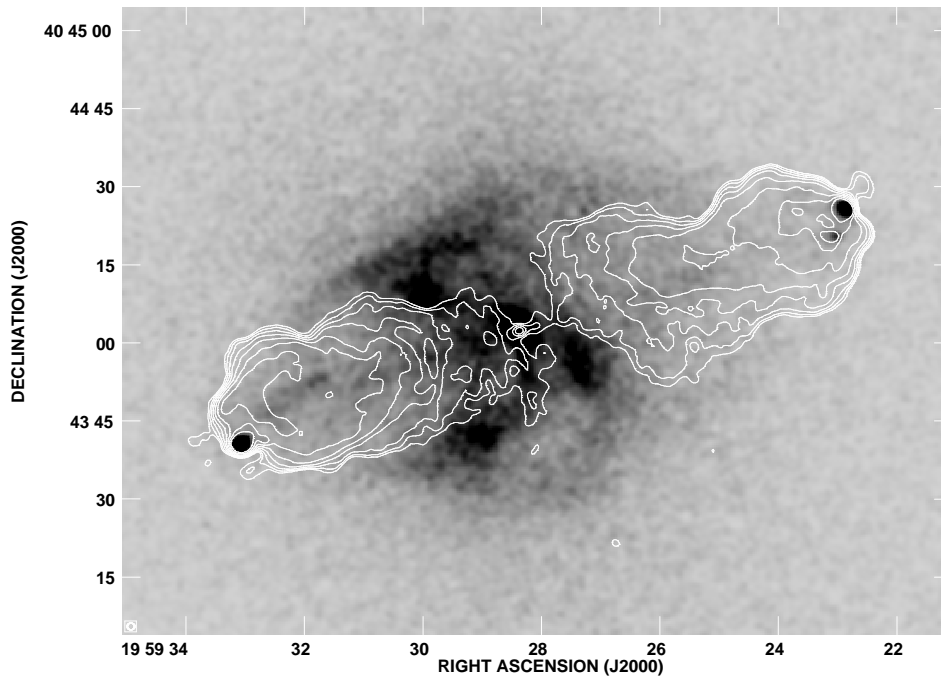


Fig. 2. The grey scale shows total Xray emission from the inner 200 kpc of the Cygnus A cluster as seen by Chandra (Smith et al. 2002). The contours show the VLA image of the radio source at 1.4 GHz.

including emission from the unperturbed atmosphere (see above), plus excess emission from the shocked ICM surrounding the radio lobes, and a deficit of emission from the evacuated radio lobes themselves. A critical aspect of this process is the temperature dependence of Xray emission, ie. the detected Xray emission will depend strongly on the observed energy band, the temperature of the external medium, and the strength and evolution of the bow shock (Clarke et al. 1997).

Figure 2 shows the radio image of Cygnus A plus the Chandra image of the inner 200 kpc of the Cygnus A cluster (Smith et al. 2002). This image shows clearly the interaction of the radio source and the cluster gas, including deficits of Xray emission at the positions of the radio lobes, and excesses of emission directly surrounding the radio lobes.

As a probe of thermal processes, Xray observations provide direct constraints on physical conditions in the emitting regions. In contrast, observations of nonthermal radio synchrotron radiation provide only indirect physical probes requiring many assumptions (eg. minimum energy). Smith et al. (2002) have considered the pressure in the shocked thermal material enveloping the radio lobes in Cygnus A, for which they derive a pressure of  $\sim 1 \times 10^{10}$  dyne  $\text{cm}^{-2}$ . For comparison, the minimum pressure in the radio lobes derived from the synchrotron surface brightness is  $2 \times 10^{11}$  dyne  $\text{cm}^{-2}$ . Given that the shocked fluids must be in pressure equilibrium along the contact discontinuity, this difference suggests a departure from minimum energy conditions in the radio lobes by a factor five.

## 2.2 Nonthermal emission

Figure 2 also reveals Xray emission coincident with the radio hot spots in Cygnus A. The spectral analysis of Wilson et al (2000) shows that this Xray emission is consistent with nonthermal IC emission from the same population of relativistic electrons emitting radio synchrotron radiation. In this case the dominant radiation field is the radio synchrotron photons themselves, such that the emission has been called synchrotron self Compton (SSC) emission (Harris et al. 1994).

Given a photon field, the IC Xray emissivity constrains the number density of relativistic electrons, while the radio emissivity is a function of the relativistic electron density and the magnetic field strength. A comparison of the two then provides an estimate of the magnetic field strength. Wilson et al. (2002) derive fields of  $150 \mu\text{G}$  for the radio hot spots based on the SSC and synchrotron emissivities. The minimum energy fields in the hot spots are about  $250 \mu\text{G}$ , suggesting that the physical conditions in the hot spots are not far from minimum energy.

An important point to keep in mind in this regard is the increase in the energy density of the microwave background with redshift ( $U_{\text{CMB}} = 4.2 \times 10^{-13}(1+z)^4$  erg  $\text{cm}^{-3}$ ). Figure 1B shows the evolution of  $U_{\text{CMB}}$  with redshift versus the typical magnetic energy densities in galaxies and radio galaxies. The implication is that in the disks of normal galaxies IC losses off the CMB will dominate over synchrotron losses for galaxies beyond  $z \sim 1$ . The cross

over point for radio lobes is  $z \sim 3$ , while that for radio hot spots is  $z \sim 7$ .

The increasing significance of IC losses with redshift has led some to hypothesize the possibility of IC-loud, but radio quiet, jets at high redshift (Schwartz et al. 2002). The important point is that the spectral peak of the CMB behaves as  $1.6 \times 10^{11}(1+z)$  Hz, such that observations at 1 keV are sensitive to electrons with  $\gamma_e \sim 1000$ , independent of redshift. The radiative lifetime of such electrons at  $z \sim 6$  is about  $1 \times 10^7$  years. For comparison, observations of a  $z = 6$  jet at 1.4 GHz probe electrons with  $\gamma_e \sim 7000$ , corresponding to radiative lifetimes of  $2.5 \times 10^6$  years.

### *2.3 Xrays from the obscured AGN*

Cygnus A shows a hard, highly obscured nuclear Xray source with  $N(\text{HI}) = 2 \times 10^{23} \text{ cm}^{-2}$ ,  $\Gamma = 1.5$ , and  $L_{2-10\text{keV}} = 1.2 \times 10^{45} \text{ erg s}^{-1}$  (Young et al. 2002). Young et al. (2002) also find evidence for a scattered Xray component with a luminosity of about 1% of the nuclear Xray source. The scattered component is co-spatial with the high ionization optical line emitting regions, supporting the idea that these regions are photo-ionized by radiation from the AGN.

As a matter of completeness, there have been Chandra observations of a number of other luminous radio galaxies at  $z \sim 0.5$  (Harris et al. 2002; Hardcastle et al. 2002). These observations reveal similar phenomena as those seen in Cygnus A, although not in such exquisite detail.

## **3 Xray observations of high redshift radio galaxies**

### *3.1 Cluster atmospheres and AGN emission*

Four high redshift powerful radio galaxies have been observed with Chandra to date: 1138–262 at  $z=2.2$ , 0236–254 at  $z = 2.0$ , 3C 294 at  $z = 1.8$ , and 0902+343 at  $z=3.4$ . All were detected, and all but 0902+343 show spatially extended Xray emission (Figure 3; for 3C 294 see Crawford this volume; for 0902+343 see Fabian et al. 2002). The emission mechanisms appear to span the full range of thermal and non-thermal processes seen at low redshift, and I will consider each in turn.

One of the primary drivers for observing high redshift radio galaxies in the Xray was to search for large scale structure (ie. hot cluster atmospheres) at high redshift, with the potential to place stringent constraints on  $\Omega_M$  (Fabian et al. 2001). The sources listed above were all chosen because they showed

clear evidence for being situated in dense cosmic environments (large Ly  $\alpha$  halos and galaxy overdensities, extreme rotation measures, highly disturbed radio morphologies, etc...).

While three of the sources show spatially extended Xray emission, in no case do we find evidence for a massive cluster atmosphere. Typical limits to the luminosity of cluster atmospheres associated with these sources are  $L_{2-10\text{keV}} < 2 \times 10^{44} \text{ erg s}^{-1}$ .

Considering clustering, in one source (1138–262), Pentericci et al. (2002) have found an excess of Xray loud AGN in vicinity of the radio source, by a factor two relative to the field. Six of these sources are spectroscopically or photometrically confirmed to be at the redshift of the radio galaxy.

Xray emission is detected from the nuclei of all the sources observed thus far. The data are consistent with highly obscured powerlaw spectra with:  $L_{2-10\text{keV}} \sim 2 \times 10^{45} \text{ erg s}^{-1}$ ,  $\Gamma \sim -1.5$ , and  $N(\text{HI}) \sim 1 \times 10^{-23}$ . The implied visual extinction is about  $A_V \sim 60$  assuming a Galactic dust-to-gas ratio. The ratio of the core radio to Xray luminosities for these sources are within the range defined by steep spectrum radio loud quasars. Using the relationship between core Xray luminosity and bolometric QSO luminosity, the implied bolometric luminosities for these AGN are between  $10^{46}$  to  $10^{47} \text{ erg s}^{-1}$  (Brinkmann et al. 1997).

### 3.2 *Radio-Xray alignment effect*

The most surprising aspect of the Xray observations of high redshift radio galaxies is that the extended Xray emission is closely aligned with the radio axis, and on a similar scale (Figure 3; see also Crawford this volume). Like the radio-optical alignment effect for high  $z$  radio galaxies, it appears that multiple mechanisms may be responsible for the radio-Xray alignment effect.

One possible mechanism is the West/Barthel-Arnaud effect (West 2000; Barthel & Arnaud 2000). The basic idea is that galaxies form along filamentary structures, and that radio jets propagating along the axis of highest density have higher conversion efficiency of jet kinetic energy into radio luminosity. The original thermal interpretation of the Xray emission in 3C 294 by Fabian et al. (2001) would be consistent with this model, although more recent data has called this original interpretation into question (see Crawford this volume).

A second mechanism is non-thermal radiation, either synchrotron or IC. For 2036–254 (Figure 3) the Xray emission coincides with the inner part of the radio lobe situated closest to the nucleus (presumably the receding radio lobe). The Xray and radio emission show opposite gradients, with the Xrays de-

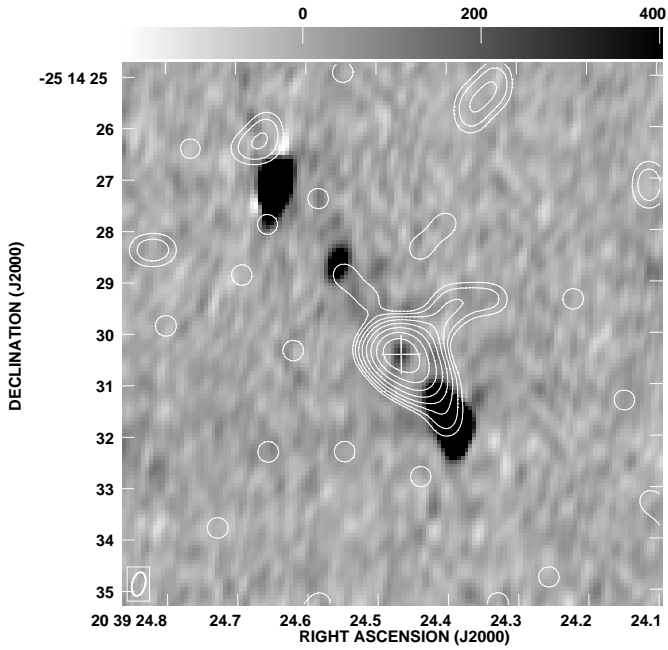
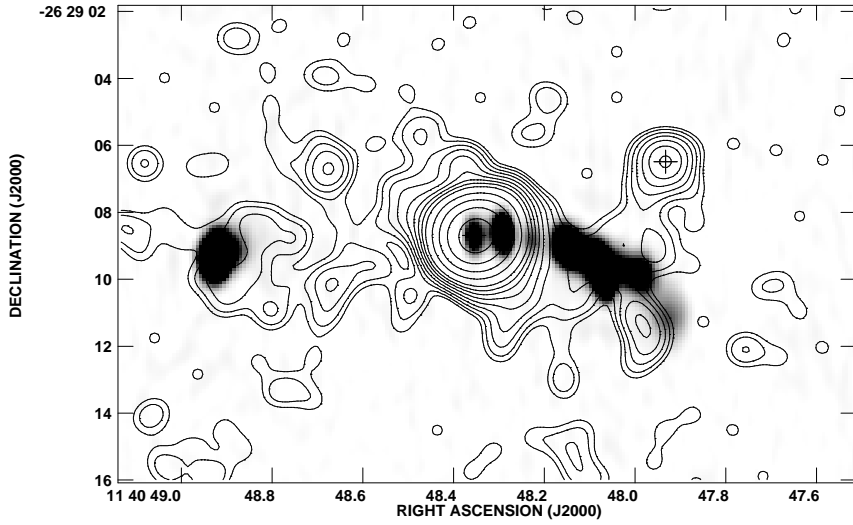


Fig. 3. Top: The contours show the Xray emission from PKS 1132–262 and the greyscale shows the radio emission at 5 GHz (Carilli et al. 2002). Bottom: The contours show the Xray emission from 2036–254 and the greyscale shows the radio emission at 8 GHz.

creasing with increasing distance from the nucleus, while the radio increases. This morphology is consistent with the Brunetti mechanism of IC scattering of radiation from the AGN by the relativistic electrons in the radio source (Brunetti 2000).

For 2036–254 it can be shown that the energy density in the radiation field is dominated by photons from the active nucleus within about 10 kpc of the AGN, assuming an AGN luminosity of  $10^{46}$  erg s $^{-1}$  (as opposed to the CMB and the radio synchrotron photons). Moreover, Brunetti (2000) predicts that the receding lobe will be brighter in Xrays than the approaching lobe both because it is closer to the nucleus (due to the time delay) and because back-scattering is more efficient than forward-scattering. Comparing the IC Xrays and the synchrotron radio emission implies a magnetic field of 25  $\mu$ G is the radio source, which is a factor three below minimum energy.

The most spectacular example of the radio-Xray alignment effect is PKS 1138–262. This source has been considered in detail by Carilli et al. (2002). They find that multiple mechanisms may be at work in 1138–262. Emission from the radio galaxy AGN, and a second AGN about 6" to the northwest is detected. The Xray emission from the inner radio jet is most likely due to the Brunetti mechanism described above, with implied magnetic fields of about 30 $\mu$ G.

For the outer radio jet the most plausible mechanism is thermal emission from gas shock heated by the expanding radio source. The implied parameters for the thermal gas are:  $n_e = 0.05$  cm $^{-3}$ ,  $M_{\text{gas}} = 2.5 \times 10^{12}$ , and  $P_{\text{gas}} = 8 \times 10^{-10}$  dynes cm $^{-2}$ . The pressure in the Xray emitting gas is comparable to that in the (low filling factor) optical line emitting gas, and to minimum pressures in the radio source. Chambers et al. (1990) first pointed out the need for a high filling factor, hot gas to confine the optical line emitting gas and the radio source in high redshift radio galaxies.

Rees (1989) suggested that the ambient medium into which a radio jet propagates may be very different for high redshift sources relative to low redshift sources. For the low redshift sources the medium is a relatively smooth, virialized ( $10^8$  K) cluster atmosphere. For the high redshift sources such a smooth medium has not had time to develop. The ambient medium is likely to be multiphase, with structures ranging from low filling factor, high density ( $>$  few cm $^{-3}$ ), cold ( $10^4$  K) clouds, to high filling factor, lower density ( $<$  0.01 cm $^{-3}$ ) regions at the virial temperature of  $10^6$  to  $10^7$  K. The passage of a radio jet through such a multiphase medium will lead to a number of interesting phenomena (Kaiser & Alexander 1999). The high density clouds are induced to form stars due to the higher pressure environment. The intermediate density regions are shocked, but cool on timescales comparable to the radio source lifetime ( $10^7$  years), and emit Ly  $\alpha$  radiation. The lower density, higher filling factor gas is shock heated to Xray emitting temperatures. The Chandra observations of 1138–262 may have revealed, for the first time, this hot and pervasive medium, as required to confine the radio source and the optical line clouds.

Optical observations of radio galaxies and their environments have revealed

cluster-like overdensities of galaxies (Venemans these proceedings). However, the velocity dispersions are smaller than expected for a virialized cluster. Likewise, the Xray observations of high redshift radio galaxies have shown that they are not at the center of massive, virialized cluster atmospheres, and suggest the existence of a much less mature ambient medium. Overall, these observations are consistent with the idea that high redshift radio galaxies are in proto-cluster environments, ie. regions that will evolve into dense clusters, but have not yet had time to fully separate from the Hubble flow and virialize.

This paper summarizes work done with many collaborators, including H. Rottgering, D. Harris, L. Pentericci, G. Miley, R. Overzier, J. Kurk. The National Radio Astronomy Observatory (NRAO) is operated by Associated Universities, Inc. under a cooperative agreement with the National Science Foundation. This research was supported by a grant from the Chandra observatory, and made use of the Chandra archive.

## References

- [1] Barthel, P. & Arnaud, K. 1996, MNRAS, 283, L45
- [2] Brinkmann, W. et al. 1997, A& A, 319, 413
- [3] Brunetti G. 2001, APh, 13, 107
- [4] Carilli, C.L. & Barthel, P.D. 1996, Astro. Astrophys. Review, 7, 1
- [5] Carilli, C.L. et al. 2002, ApJ, 567, 781
- [6] Carilli, C.L., Perley, R.A., & Harris, D.E. 1994, MNRAS, 270, 173
- [7] Chambers, K, Miley, G., & van Breguel, W. 1990, ApJ, 363, 21
- [8] Clarke, D.A., Harris, D.E., & Carilli, C.L. 1997, MNRAS, 284, 981
- [9] Fabian, A., Crawford, C., Ettori, S., & Sanders, J. 2001, MNRAS, 322, L11
- [10] Fabian, A., Crawford, C., & Iwasawa, K. 2002, MNRAS, 331, L57
- [11] Hardcastle, M. et al. 2002, ApJ, in press
- [12] Harris, D. et al. 2000, ApJ, 530, L81
- [13] Harris, D.E., Carilli, C.L., & Perley, R.A. 1994, Nature, 367, 713
- [14] Kaiser, C. & Alexander, P. 1999, MNRAS, 305, 707
- [15] Pentericci, L. et al. 2002, A& A, in press
- [16] Rees, M. 1989, MNRAS, 239, 1P
- [17] Reynolds, C. & Fabian, A.C. 1996, MNRAS, 278, 479
- [18] Schwartz, D. 2002, ApJ (letters), in press
- [19] Smith, D.A. et al. 2002, ApJ, 565, 195
- [20] Ueno, S. et al. 1994, ApJ, 431, L1
- [21] West, M. 1999, in The Most Distant Radio Galaxies, eds. Rottgering, Best, & Lehnert (Amsterdam: Royal Netherlands Acad.), 365
- [22] Wilson, A.S., Young, A.J., & Shopbell, P.L. 2000, ApJ, 544, 27L
- [23] Young A.J. et al. 2002, ApJ, 564, 176